High lift analysis for unmanned aircraft LAPAN surveillance UAV (LSU)-05 NG

Cite as: AIP Conference Proceedings **2226**, 030013 (2020); https://doi.org/10.1063/5.0002339
Published Online: 22 April 2020

M. L. Ramadiansyah, A. B. Utama, P. A. P. Suseno, R. A. Ramadhan, K. Hidayat, A. Septiyana, A. Rizaldi, N. Atmasari, and E. B. Jayanti

High Lift Analysis for Unmanned Aircraft LAPAN Surveillance UAV (LSU)-05 NG

M. L. Ramadiansyah[1,a)], A. B. Utama[1,b)], P. A. P. Suseno[1,c)], R. A. Ramadhan[1,d)], K. Hidayat[1,e)], A. Septiyana[1,f)], A. Rizaldi[1,g)], N. Atmasari[1,h)], and E. B. Jayanti[1,i)]

[1]*Aeronautics Technology Center, LAPAN, Indonesia*

[a)]Corresponding author: mohamad.luthfi@lapan.go.id
[b)]agus.bayu@lapan.go.id [c)]prasetyo.ardi@lapan.go.id [d)]redha.akbar@lapan.go.id [e)]kurnia.hidayat@lapan.go.id
[f)]angga.septiyana@lapan.go.id [g)]ardian.rizaldi@lapan.go.id [h)]novita.atmasari@lapan.go.id [i)]eries.bagita@lapan.go.id

Abstract. LAPAN Surveillance Aircraft (LSU)-05 NG is the latest developed unmanned aircraft in the aviation industry, which has a mission for maritime surveillance. Design requirements and objectives have been determined for the aircraft performance. Some improvement of the design needed to achieve the requirement and to get the optimum aerodynamic performance, including to determine the high lift device design. The selection of suitable high lift device type for UAV LSU-05 NG model has been made and also the numerical analysis using CFD for 2D and 3D at wing level has been performed to get the optimum design of high lift device. The selection of HLD type also considered of simplicity of manufacturing and mechanism by qualitative. Finally, the high lift device type which has an optimum performance for unmanned aircraft is plain flap-type with a 10.20% lift increasing at 15 m/s stall speed at take-off compared to the wing configuration without flap. The final configuration has the runway prediction with 170 m distance, which is within the requirement.

INTRODUCTION

Takeoff is the starting phase of a flight of an aircraft. Takeoff and landing are the most significant phase of aircraft operation because the majority of aircraft accidents occurs during these two phases.1 An aircraft need the high lift during low speed while in the takeoff phase to compensate for the maximum takeoff weight. If we can increase the maximum lift coefficient it is also related to the high performance of aircraft weight, and cost as well because the performance of an airplane is strongly related to every part of airplane design and operation.2 At the low speed, an aircraft has a lift coefficient of around 1.4 to 1.5 generally. The development of variable camber devices of the wing allows the aircraft to improve the aerodynamic performance by changing the wing curvature under different flight conditions.3 It can be applied high lift devices at the leading edge and trailing edge of the wing, namely flap. The factors which affect the decision of flap size and type are high lift requirement, trim considerations, drag considerations, cost, complexity, and maintenance.4 The leading edge flap has two types such as Kruger and Slat, while for the trailing edge flap-type are a Plain, Split, Fowler, and Slotted.

Aeronautics Technology Center of LAPAN (National Institute of Aeronautics and Space) Indonesia is developing unmanned aircraft called LAPAN Surveillance UAV (LSU)-05 NG with configuration high wing, twin tail boom and engine pusher for a maritime surveillance mission.5 Since 1917, when the first UAV (Unmanned Air Vehicle) was developed successfully in England, It has been progressing through several stages, which are target drone, reconnaissance aircraft, and multi-role UAV. Also, it has been successfully useful for military purpose in four local wars, which has come to the attention of the world.6 The specific requirement for the takeoff phase of the LSU-05 NG aircraft is the stall speed not exceed than 18 m/s and the runway distance is 180 m or lower with maximum takeoff weight is 75 kg. This requirement related to application at the patrol ships. Regardless of the specific UAV configuration, engineers are required to design UAVs that can successfully withstand a wide range of flight conditions, are suitable for long survey periods and have the advantage of low cost.7 To optimize the takeoff and landing

7th International Seminar on Aerospace Science and Technology – ISAST 2019
AIP Conf. Proc. 2226, 030013-1–030013-10; https://doi.org/10.1063/5.0002339
Published by AIP Publishing. 978-0-7354-1985-8/$30.00

performance and meet the requirement, the designer needs to analyze the high lift devices that will be determined in this paper. Due to the iterative nature of design, it is important for designers to evaluate with good confidence the control authority of candidate concepts as early as possible in the design process. Normally numerous possible configurations are considered before the stability and control specialists start their analysis for the detailed control system design.[8]

In order to determine the best design, numerical analysis is used to evaluate the behavior of multiple candidates, which one with the top performance in terms of the desired objective is selected.9 There are so many efforts to solve the design problem of high-lift devices aerodynamics. The wind tunnel data is a good guidance for those who are researching and designing high-lift devices aerodynamics. However the wind tunnel systems are too complex and expensive. That is why these days many researchers and designers use Computational Fluid Dynamics (CFD). The maximum lift coefficient is able to obtain in a reasonably short amount of time.2 Considering its capabilities 10–15 years ago, CFD has come a long way toward becoming a useful tool for the design and analysis of 3-D high-lift aerodynamic systems.[10] High lift selection also considered to simplicity of manufacturing and mechanism by qualitative with some references of research by LAPAN and Weishuang in Ref. 11. While the earlier effort of high-lift system design was mainly on enhancing the maximum lift, the later trend turned to reduce the complexity, weight and maintenance costs for a given maximum lift level.[12]

METHODOLOGY

High lift optimization is composed of 6 steps that shown in Fig. 1. This optimization consists the analysis of aerodynamics using CFD. Computational Fluid Dynamics (CFD) is becoming increasingly popular in the design and optimization of devices that depend on aerodynamics.[14]

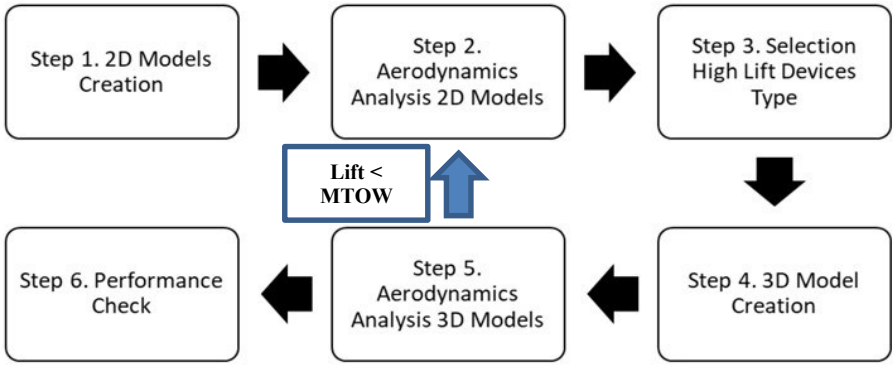

FIGURE 1. Methodology Steps for Optimization High Lift Devices

Step 1 consists of the creation of 2D models for some types of flap with the airfoil. The CFD analysis to get the aerodynamic performance needs the geometry first. The 2-dimensional analysis should be done for high lift device selection to get an efficient time from 3D calculation. Step 2 consists of the CFD process of 2D models of the flaps. The calculation must be done with a grid test before the calculation would be going. The grid test purpose is to minimize the residual result from the CFD results compared to experimental tests such as a wind tunnel test. Step 3 consists of the high lift devices type selection process. This process depends on the analysis of aerodynamic characteristics and also the complexity of the mechanism. The main purpose is to get a high-performance device with a low effort of manufacturing. Step 4 consists of the creation of 3D models. This creation also including the no flap configuration to know the characteristic without flap thus would be seen the different performance between no flap and with flap configurations. Step 5 consists of the CFD process for the 3D model and aerodynamics analysis. In this step also would be calculated the maximum weight that can be lifted by wing configurations. The looping calculation is possible when the lift of 3D model does not meet the MTOW requirement at the defined stall speed, thus increases the stall speed and begin with the 2D analysis. Step 6 consists of the performance check to know the takeoff and the landing ground estimated distance, so it would be seen that the optimization affected by runway distance and would be compared to the requirement which has been determined.

IMPLEMENTATION

All steps have been implemented following the below section. In this paper, some steps were merged to easier for analysis, such as HLD type selection contained in the CFD 2D Model and 3D model creation merged with aerodynamic analysis 3D. All information and data would be presented in each section of this paper.

2D Model Creation

The flap-type which has a simple mechanism and suitable to UAV size is plain, split and slotted. Flap model creation follows the airfoil FX 76-MP-160 that has been selected for LSU-05 NG wing airfoil. The chord length follow the root size of the wing with 730 mm length and the model of selected flaps can be shown in Figs. 2(b)-2(d). It also shown the model of airfoil without flap for comparison in Fig. 2(a).

(a) (b) (c) (d)

FIGURE 2. 2D Geometry Model of Airfoil FX 76-MP-160: a. No Flap, b. Split Flap, c. Plain Flap, d. Slotted Flap

The length of all flaps are quarter from a trailing edge of airfoil 182.5 mm, this is a fixed parameter from the requirement and should be determined so it can be comparable. And also the deflection of the flap has been defined fixed at 30 deg. For slotted flap was built with an expansion of 63 mm in the backward direction and no change in the vertical direction. The geometry generation is the first task carried out in the developed design framework.8 The boundary area is quite larger than the geometry, it has 10 m x 6 m size with 3 m distance from the front, top, and bottom layer. The mesh generation of the computational model is then carried out in the ANSYS Mesh.[13] The unstructured mesh was applied in this step with face sizing on the surface 1 mm and relevant -25%. This configuration is the most efficient mesh considering to total element and simulation time that was confirmed by the grid test. Mesh results can be seen in Fig. 3(a)-3(d).

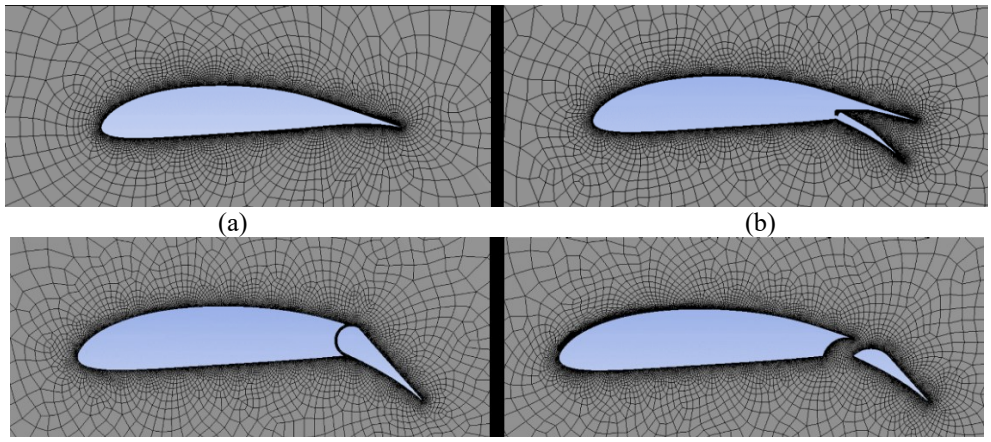

(a) (b)

(c) (d)

FIGURE 3. Generated Mesh for 2D Airfoil Model: a. No Flap, b. Split Flap, c. Plain Flap, d. Slotted Flap

CFD 2D Model

To process the calculation, the simulation parameter has been determined that can be shown in table 1.

TABLE 1. Simulation Parameter

Parameter	Value
Air Density	1.185 kg/m^3
Airspeed	15 m/s
Angle of Attack	-15 to 20 deg with interval 5 deg
Air Pressure	1 atm

An airspeed that used in this calculation is 15 m/s which still far from the requirement, this is the first assumption parameter and can be changed if the lift generation is still low. If the lift generation was achieved at this airspeed, it would be impacted by the runway distance to become shorter. The simulation is done with a variable angle of attack to determine aerodynamic coefficients such as lift and drag. The streamline of the CFD result can be shown in Fig. 4(a)-4(d) that was collected at the angle of attack 15 deg.

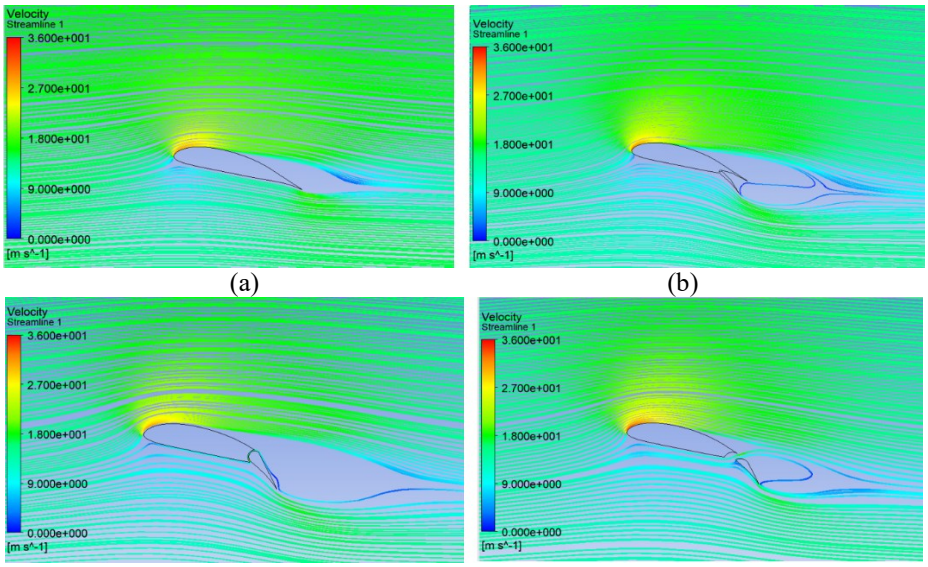

FIGURE 4. Streamline at Airfoils at AoA 15 deg: a. No Flap, b. Split Flap, c. Plain Flap, d. Slotted Flap

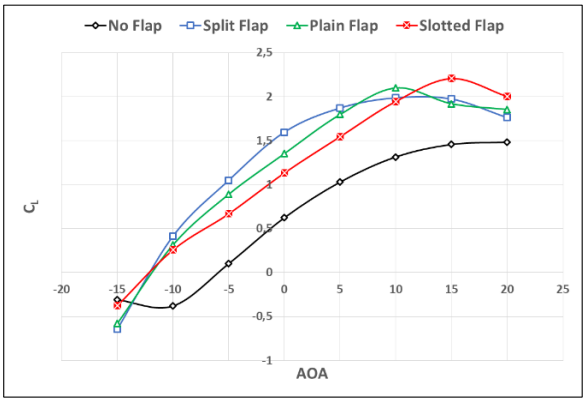

FIGURE 5. Lift Coefficient vs AoA 2D Model

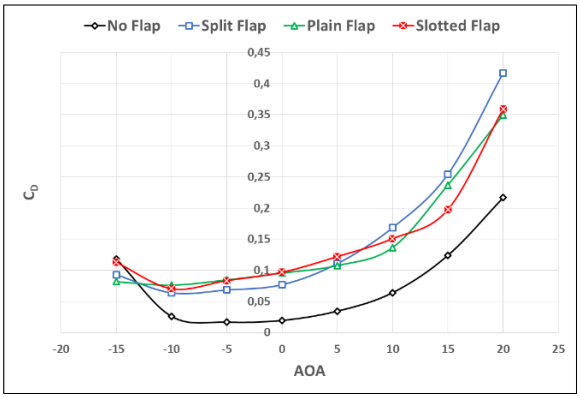

FIGURE 6. Drag Coefficient vs AoA 2D Model

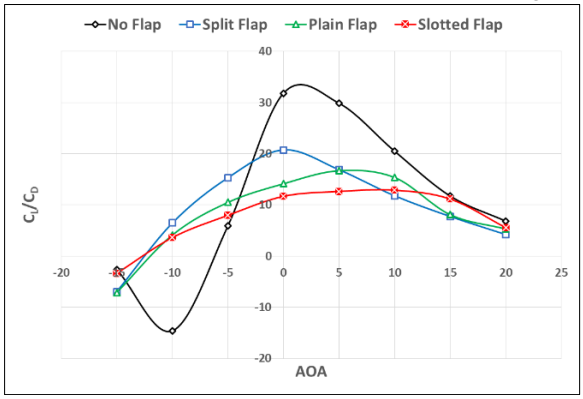

FIGURE 7. Lift/Drag vs AoA 2D Model

From the lift coefficient trend in Fig. 5, it can be seen that the slotted flap has the highest $C_{L,max}$ compared to the plain-flap and split-flap at AoA 15 deg which is the value is 2.20. In Fig. 5, also can be seen $C_{L,max}$ of the plain flap is the highest at the lower AoA 10 deg with the value 2.09. From this point, the decision was chasing the plain flap as the high lift device type because it has the $C_{L,max}$ at the lower AoA, 10 deg. The 2D model has assumed that the span of the airfoil and flap is infinite length, after did 3D model, the AoA of the stall condition will be expanded to the higher AoA. And also it just has a slightly different with the $C_{L,max}$ of the slotted flap. From the drag coefficient in Fig. 6, it can be seen that at 10 deg AoA, the plain flap has the lowest CD compared to all flap configurations. In Fig. 7 shown the CL/CD vs AoA that belong to aerodynamic efficiency, it is shown that plain flap has the highest efficiency at AoA 10 deg between all flap configurations. Compared also with the manufacturing process and mechanism qualitatively, the plain flap has simpler than slotted flap. The effort between the lift generation and the production of the plain and slotted flap decided to chase the plain flap. Thus, the 3D model continues with the plain flap type.

Analysis for 3D Model

A 3D-panel method was used for this analysis, modeling the wake as a series of flat panels which extend 'far behind' the wing.[15] The 3D model geometry has been determined only for half wing configuration. This geometry defined considered to the final fuselage and another component of aircraft that has not been determined yet, so the aerodynamic performance belongs to the wing. Since the wing is the main lift generation of aircraft components, the value of the lift coefficient assumed near the lift coefficient of the full geometry of the aircraft. To make the short time simulation, it performed with a half section since the parameter just looked for lift and drag coefficient, therefore the simulation could be done efficiently. The configuration is contained inner and outer flaps because the aircraft configuration will be assembled tail boom to the wing. There are 3 geometries that will be done the simulation, the wing configuration only without flap, wing configuration with flap and wing configuration with flap and flaperon that can be seen in Fig. 8(a)-8(c). The 3D model also puts the flaperon as the additional geometry configuration for prevention design while the lift generation of flap configuration in takeoff condition is still low. The 3D meshing result has been performed that shown in Fig. 9(a)-9(c).

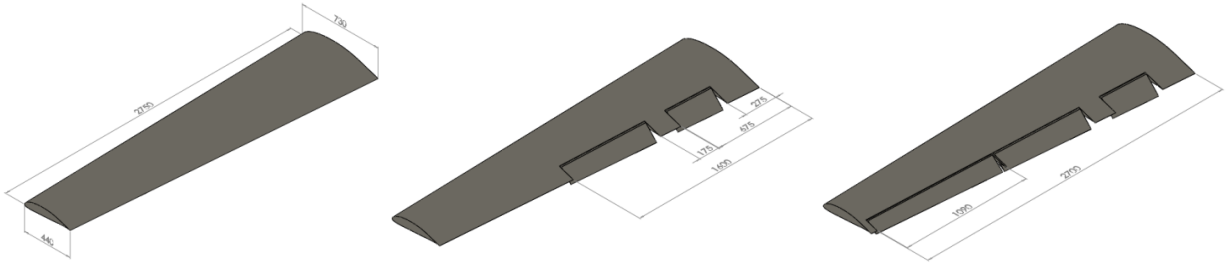

(a) (b) (c)

FIGURE 8. 3D Geometry Model of Wing Configuration: a. No Flap, b. Plain Flap, c. Flap and Flaperon

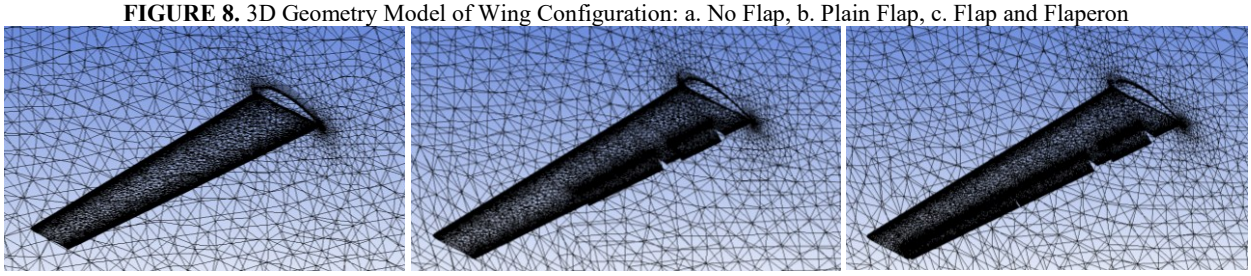

(a) (b) (c)

FIGURE 9. Generated Mesh for 3D Model: a. No Flap, b. Plain Flap, c. Flap and Flaperon

In Fig. 8(a)-8(c) also shown the dimension of a chord length in the root and edge wing, length of flap and flaperon slot. The dimension of an inner flap, outer flap, and flaperon itself has the gap 5 mm to the wing surface for all sides. In Fig. 9(a)-9(c) can be seen the mesh modeling used unstructured mesh with additional inflation for all surfaces of the wing. The streamline of the CFD 3D model result at AoA 15 deg shown in Fig. 10(a)-10(c).

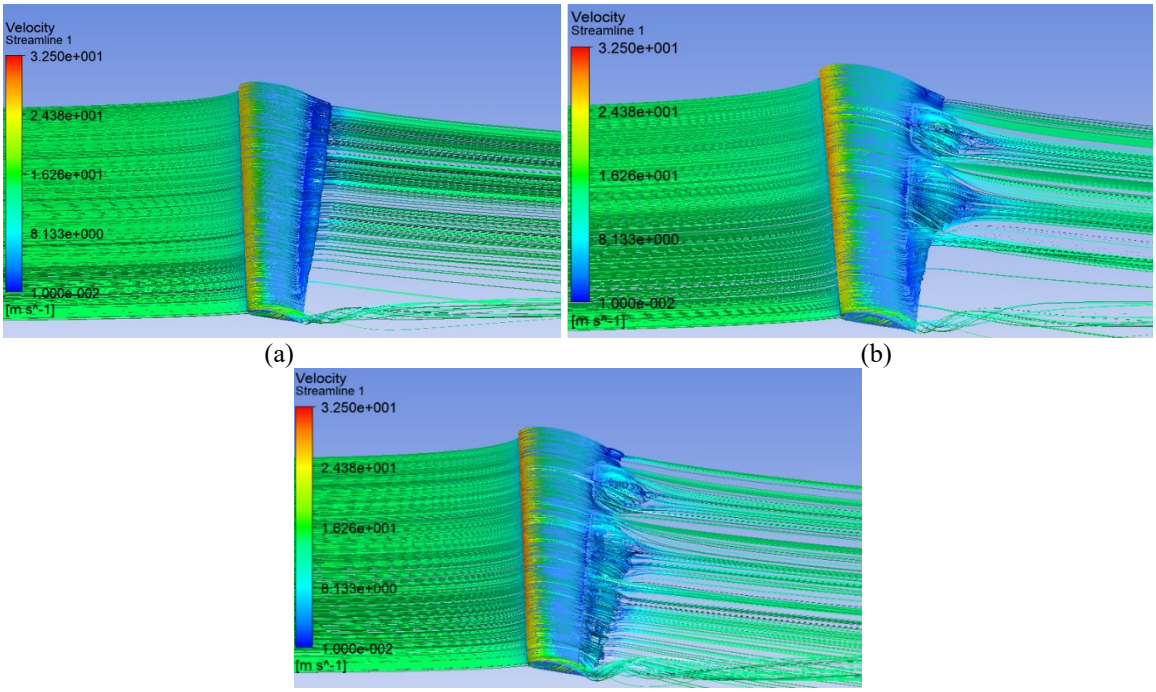

FIGURE 10. Streamline at Wing AoA 15 deg: a. No Flap, b. Plain Flap, c. Flap and Flaperon

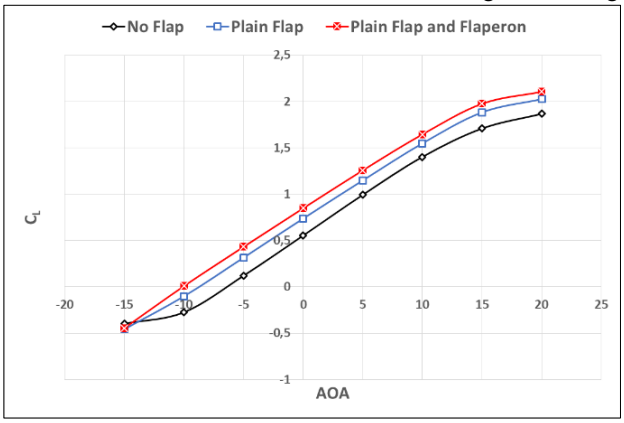

FIGURE 11. Lift Coefficient vs AoA 3D Model

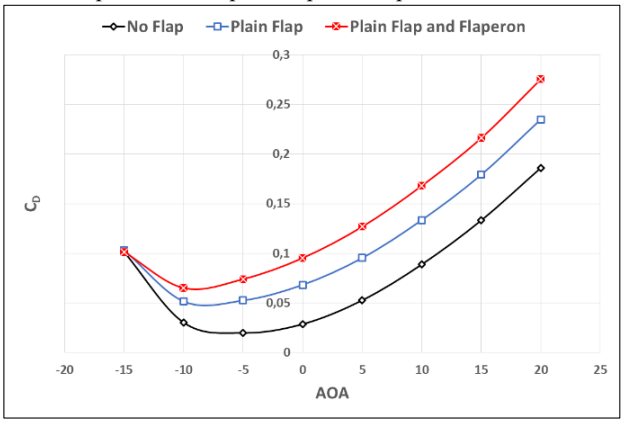

FIGURE 12. Drag Coefficient vs AoA 3D Model

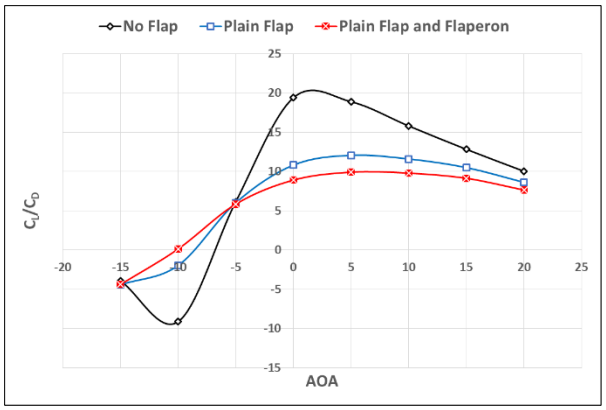

FIGURE 13. Lift/Drag vs AoA 3D Model

The 3D simulation parameter as the same as the 2D model. As can be seen in Fig. 10, the streamline becomes turbulences behind the flap and flaperon which means there will be an additional induce drag caused by additional high lift devices. The result of the lift coefficient (in Fig. 11) and drag coefficient (in Fig. 12) has been determined, it can be seen that the maximum lift coefficient is higher than 10 deg as expected at 2D simulation analysis. The lift coefficient is still going up referred to Fig. 11 and shown the curve would turn down at AoA around 20 deg, the maximum AoA operation that defined from the design requirement is 15 deg, so the aerodynamic parameter taken from AoA 15 deg. At this point, the drag coefficient of flap wing configuration has slightly different with no flap configuration shown in Fig. 12. It was shown in Fig. 13 that the aerodynamic efficiency at 15 deg is slightly different. The analysis of lift generation can be seen below. It has been determined followed Eq. (1) that taken from the lift equation,

$$L = \frac{1}{2}\rho S C_L V^2 \tag{1}$$

With ρ for air density = 1.185 kg/m^3; S for span area of the wing = 3.2175 m^2; V for airspeed = 15 m/s. The MTOW also has been calculated following Eq. (2) with g for gravity = 9.81 m/s^2. Thus got the value of lift generation and the ratio compared to the no flap configuration in table 2.

$$m_{MTOW} = \frac{L}{g} \tag{2}$$

TABLE 2. Lift and MTOW Calculation at 15 m/s and AoA 15 deg

Configuration	C_L	Lift (N)	MTOW (kg)	Ratio (%)
No Flap	1.71	732.71	74.69	-
Plain Flap	1.88	807.48	82.31	10.20
Plain Flap and Flaperon	1.97	847.22	86.36	15.62

As shown in table 2, the plain flap configuration has fulfilled the MTOW requirement. The lift generation from plain flap configuration has 7 kg tolerance from the requirement, so it could be considered the full aircraft configuration since this analysis only performed at the wing level. A flaperon configuration was not required since the flap configuration already meets the requirement.

Runway Performance Prediction

The distance of the runway has been calculated referred to the aerodynamic parameter such as lift and drag coefficient from the CFD result of the 3D model wing with plain flap configuration. The calculation formula is taken from Ojha1 consist the performance of the takeoff and landing phase of the aircraft. All data were given as shown in table 3.

TABLE 3. Takeoff and Landing Data

Parameter	Symbol	Value
Wing Span Area	S	3.2175 m^2
Engine Power	P	15 hp
Propeller Efficiency	η_p	85 %
Maximum Takeoff Weight	m_{MTOW}	80 kg
Maximum Landing Weight	m_{MLW}	75 kg
Maximum Lift Coefficient	$C_{L,max}$	1.88
Drag Coefficient at $C_{L,max}$	$C_{D,m}$	0.18
Stall Speed	V_S	15 m/s
Average Deceleration	$\bar{d}$	$0.55g$
Approaching Angle	γ_{Ap}	5 deg
Surface Control Height	h_{SC}	15.24 m
Air Density	ρ	1.225 kg/m^3
Dynamic Friction Coefficient	μ	0.8
Gravity	g	9.81 m/s^2

Takeoff

In this phase, there were 4 steps that should be analyzed: ground roll, rotation, transition and takeoff climb that shown in Fig. 14. According to table 3 as the parameter that known for calculation. Thus, following the Eq. (3) got the result of takeoff runway distance,

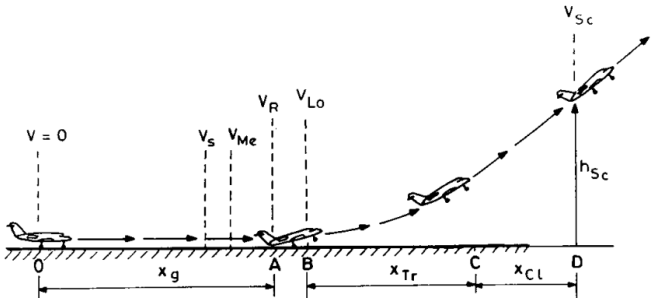

FIGURE 14. Characteristic Distances of Takeoff Phase[1]

$$x_{Rw,To} = x_g + x_R + \frac{1}{2}\left(x_{Tr} + x_{Cl}\right) \tag{3}$$

with $x_{Rw,To}$ for the takeoff runway distance; x_g for the ground roll distance that can be determined following Eq. (4); x_R for the rotation distance that can be determined following Eq. (5); x_{Tr} for the transition distance that refers to Eq. (6); and $x_{Cl,To}$ for the takeoff climb distance that defined from Eq. (7).

$$x_g = \left\{\frac{W_{MTOW}{V_{Lo}}^2}{2g}\right\}\left\{F - D - \mu\left(W_{MTOW} - L\right)\right\}_{V=0.7V_{Lo}}^{-1} \tag{4}$$

$$x_R = V_{Lo}t_R \tag{5}$$

$$x_{Tr} = R_{Tr}\sin\gamma_{Cl} = \left(\frac{V_{Lo}^2}{0.15g}\right)\sin\gamma_{Cl} \tag{6}$$

$$x_{Cl,To} = \left(h_{sc} - h_{Tr}\right)/\tan\gamma_{Cl} \tag{7}$$

In Eq. (4) should be determined the weight of MTOW W_{MTOW}, lift off speed V_{Lo} (assumed $1.15V_S$), thrust force F, drag force D and lift force L. Thus, got the ground roll distance value, $x_g = 10.14\ m$. The rotation time is assumed 3s, thus got the value of rotation distance following Eq. (5), $x_R = 50.22\ m$. In Eq. (6) should be determined the angle of climb γ_{Cl} that was referred to Eq. (8) and also need to check the transition height h_{Tr} following Eq. (9),

$$\gamma_{Cl} = \left\{\frac{\left(\eta_P P\right)}{\left(W_{MTOW}V_{P\min}\right)}\right\} - \left\{\frac{1}{\left(0.866E_m\right)}\right\} \tag{8}$$

$$h_{Tr} = \left(1 - \cos\gamma_{Cl}\right)\left(\frac{V_{Lo}^2}{0.15g}\right) \tag{9}$$

with $V_{P_{min}} = \{(W_{MTOW}/(\rho.S)\}^{1/2}\{K/3C_{Do}\}^{1/4}$, where K and C_{Do} were got from interpolated equation of relation between C_L and C_D that obtained from CFD result with the basic equation $C_D = C_{Do} + K.C_L^2$, thus got $C_{Do} = 0.048$ and $K = 0.037$. And also need to determine maximum efficiency, $E_m = \{2(KC_{Do})\}^{-1}$. Then got the climb angle, $\gamma_{Cl} = 0.755\ rad$. Eq.6 can be used if $h_{Tr} < h_{SC}$, thus check the value of transition height which following Eq. (9), thus got the transition height, $h_{Tr} = 51.81\ m$. While the transition height is larger than surface control height, then the transition distance following Eq. (10),

$$x_{Tr} = \frac{h_{sc}}{\tan\gamma_{sc}} \tag{10}$$

with the angle to reach surface control height, $\gamma_{SC} = (h_{SC}/h_{Tr})\gamma_{Cl}$. Thus, from Eq. (10) got the transition distance, $x_{Tr} = 67.49\ m$. Since the transition step was reached the surface control height, so the takeoff climb distance $x_{Cl,To}$ was negligible. From the Eq. (3), the runway distance regarding to the takeoff performance is $x_{Rw,To} = 94.11\ m \approx 95\ m$.

Landing

Landing is called the slowed-down movement of the plane from the moment of flight at the height of 15 m to the full stop or speed of taxing. The performance of landing has been calculated following Eq. (11). Landing phase is similar to the takeoff, it has 4 steps such as approach, flare, rotation landing, and ground landing that can be seen in Fig. 15,

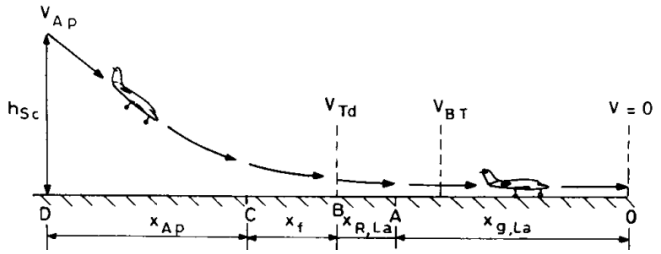

FIGURE 15. Characteristic Distances for Landing Phase[1]

$$x_{Rw,La} = \frac{1}{2}\left(x_{Ap} + x_f\right) + x_{R,La} + x_{g,La} \tag{11}$$

with $x_{Rw,La}$ for the landing runway distance; x_{Ap} for approach distance that can be determined following Eq. (12); x_f for the flare distance that can be determined following Eq. (13); $x_{R,La}$ for the rotation landing distance that refers to Eq. (14); and $x_{g,La}$ for the ground landing distance that can be defined from Eq. (15).

$$x_{Ap} = \left\{h_{sc} - \left(1 - \cos\gamma_{Ap}\right)R_f\right\} / \tan\gamma_{Ap} \tag{12}$$

$$x_f = R_f \sin\gamma_{Ap} \tag{13}$$

$$x_{R,La} = V_{Td} t_{g,La} \tag{14}$$

$$x_{g,La} = V_{Td}^2 / 2\bar{d} \tag{15}$$

The flare radius, $R_f = \left\{V_{Ap}^2/(0.08g)\right\}$, the touchdown speed $V_{Td} \cong 1.15V_{Ap}$, and the approach speed $V_{Ap} \cong 1.3V_{S,Ap}$ while the stall speed approach, $V_{S,Ap} = [2W_{MLW}/(\rho S C_{L,max})]^{1/2}$, thus the distance of approach, flare, rotation and ground landing phase are: $x_{Ap} = 155.59\ m$; $x_f = 37.26\ m$; $x_{R,La} = 48.61\ m$; and $x_{g,La} = 24.33\ m$, respectively. From the Eq. (11), the runway distance regarding to the landing performance, $x_{Rw,La} = 169.36\ m \approx 170\ m$. The runway of the landing phase is larger than the takeoff, so the runway prediction from the wing with plain flap configuration can perform at 170 m runway which is within the requirement.

CONCLUSIONS

Optimization of high lift for UAV aircraft has been done with selected high lift device type that considering the value of lift generation from 2D CFD analysis and the simplicity of the manufacturing and mechanism. The performance of this optimization has also been checked with the takeoff and landing analytical calculation which some parameters got from CFD analysis of the 3D model of wing configuration. As a result, the optimum high lift devices that can be used for UAV LSU-05 NG is a plain flap which applied for both inner and outer flap in the takeoff operation at 15 m/s. This configuration has been checked to its performance with the result of runway distance 170 m which is appropriate to the requirement of LSU-05 NG. This configuration could generate the lift for maximum takeoff weight 82.31 kg that 10.20% higher than wing configuration without flap.

This research would be excellent completed while it validated by a full configuration of aircraft and wind tunnel tests. At present, wing analysis is enough considering the lift generation of the aircraft mainly contributed by the wing. If there was applicable at the full configuration, the drag force will be increased significantly, but the lift force just slightly increased, this would be affected by the runway distance to become shorter due to the drag variable was increased.

ACKNOWLEDGEMENTS

The authors wish to express thanks to all members of the Aerodynamics Division of LSU 05-NG, Aerodynamics Laboratory, and special thanks for Mr. Gunawan Setyo Prabowo as Head of Aeronautics Technology Center and also to Mr. Atik Bintoro as our senior researcher to support this research.

REFERENCES

1. S. K. Ojha, Flight Performance of Aircraft (American Institute of Aeronautics and Astronautics, Washington DC, 1995).
2. J. Park, N.V. Nguyen, M. Tyan, S. Kim, and J.W. Lee, Flap Design Optimization for Very Light Aircraft in compliance with Airwothiness Certification (21st AIAA Computational Fluid Dynamics Conference, San Diego, CA, 2013), DOI: 10.2514/6.2013-2706.
3. Y. Tian, J. Quan, P. Liu, D. Li, and C. Kong, Mechanism/structure/aerodynamic multidisciplinary optimization of flexible high-lift devices for transport aircraft (Aerospace Science and Technology, 2019), Vol.93, 104813.
4. J. Roskam, Airplane Design Part I: Preliminary Sizing of Airplanes (Roskam Aviation and Engineering Corporation, Ottawa, 1985).
5. B. Atik, Program Manual Litbangyasa Pesawat Tanpa Awak LSU 05 NG (LAPAN, Rumpin, 2019).
6. S. Sachin and S. B. Gurram, Numerical Analysis of Wings for UAV based on High-Lift Airfoils (International Journal of Innovation in Engineering and Technology (IJIET),2015), Vol.5 Issue 3, ISSN: 2319 – 1058.
7. Y. Azabi, A. Savvaris, and T. Kipourus, Initial Investigation of Aerodynamic Shape Design Optimisation for the Aegis UAV (Transportation Research Procedia, Bucharest, 2018), Vol. 29, pp. 12-22.
8. N. Fabrizio, A. D. Marco, V. Sabetta, and P. D. Vecchia, Roll performance assessment of a light aircraft: Flight simulations and flight tests (Aerospace Science and Technology, 2018), Vol.76, pp. 471-483.
9. A. Benaouali A and S. Kachel, Multidisciplinary design optimization of aircraft wing using commercial software integration (Aerospace Science and Technology, 2019), Vol.92, pp.766-776.
10. C. L. Rumsey and S. X. Ying, Prediction of high lift: review of present CFD capability (Progress in Aerospace Science, 2002), Vol.38 Issue 2, pp.145-180.
11. L. Weishuang, T. Yun, and L. Peiqing, Aerodynamic optimization and mechanism design of flexible variable camber trailing-edge flap (Chinese Journal of Aeronautics, 2017), Vol.30 Issue 3, pp. 988-1003.
12. C. P. van Dam, The aerodynamic design of multi-element high-lift systems for transport airplanes (Progress in Aerospace Science, 2002), Vol.38 Issue 2, pp. 101-144.
13. M. Basumatary, A. Biswas, and R. D. Misra, CFD analysis of an innovative combined lift and drag (CLD) based modified Savonius water turbine (Energy Conversion and Management, 2018), Vol.174, pp. 72-87.
14. J. Morgado, R. Vizinho, M. A. R. Silvestre, and J. C. Páscoa, XFOIL vs CFD performance prediction for high lift low Reynolds number airfoils (Aerospace Science and Technology, 2016), Vol.52, pp. 207-214.
15. D. B. M. Pedro, B. B. Laura, A. G. Daniel, and D. C. M. Hernán, Aerodynamic design analysis of a UAV for superficial research of volcanic environments (Aerospace Science and Technology, 2017), Vol.70, pp. 600-614.
16. E. Ugnenko, E. Perova, Y. Voronova, and G. Viselga, Improvement of the Mathematical Model for Determining the Length of The Runway at the Stage of Aircraft Landing (10th International Scientific Conference Transbaltica 2017: Transportation Science and Technology, 2017), Vol. 187, pp. 733-741.